Polymer 49 (2008) 5053–5063

Contents lists available at ScienceDirect

Polymer

journal homepage: www.elsevier.com/locate/polymer

A novel effective way of comprising a β-nucleating agent in isotactic polypropylene (*i*-PP): Polymerized dispersion and polymer characterization

Qing-Feng Yi [a,b], Xiao-Jing Wen [a,b], Jin-Yong Dong [a,*], Charles C. Han [a,*]

[a] CAS Key Laboratory of Engineering Plastics and State Key Laboratory of Polymer Physics and Chemistry, Joint Laboratory of Polymer Science and Materials, Institute of Chemistry, Chinese Academy of Sciences, Beijing 100080, China
[b] Ph.D. Candidate of the Graduate School, Chinese Academy of Sciences, Beijing 100080, China

ARTICLE INFO

Article history:
Received 2 July 2008
Received in revised form 30 August 2008
Accepted 21 September 2008
Available online 1 October 2008

Keywords:
β-Nucleating agent
Polypropylene
Polymerized dispersion

ABSTRACT

A kind of β-nucleating agent, namely a stearic acid and stearate lanthanum complex (NAβ), was introduced into isotactic polypropylene (*i*-PP) via an in situ polymerization method for the first time. A dynamic adhesion model was constructed for interpreting the β-nucleating agent dispersion process. The effects of a polymerized dispersion of the β-nucleating agent on the content of β-crystal and crystallization behavior of *i*-PP were investigated. The results show that the crystallization peak temperature of thus β-nucleated *i*-PP was greatly increased while the spherulite size dramatically decreased compared with those of net *i*-PP. The content of β-phase (k_β value) can reach as high as 88.7% with only 0.135 wt% of NAβ addition, which holds constant with a further increase of NAβ concentration up to 3.41 wt%. The non-isothermal crystallization kinetics of thus β-nucleated *i*-PP was studied with Mo equation and crystallization activation energy estimated by Kissinger method, giving unique results pertaining to the unprecedented NAβ polymerized dispersion.

1. Introduction

Isotactic polypropylene (*i*-PP) is one of the most important thermoplastic polymers owing to its low manufacturing cost and rather versatile properties. Moreover, *i*-PP is of polymorphic composition, having at least four modifications: α,β,γ, and smectic [1–5], all sharing a threefold conformation [6–9]. The difference in the crystallography is the manner in which the chains are packed in the unit cell. The intrinsic architecture and extrinsic parameters affect mostly through their influence on crystallization behavior and morphological features, which are probably the most important factors affecting the final physical properties. Therefore, controlling the growth rate and tailoring the proportion of different polymorphs are extremely important for *i*-PP applications.

Among all the four known crystalline structures (α,β,γ, and smectic) of *i*-PP, the β-form may be the most fascinating one because of its unique structure. The β-spherulites often exhibit banded textures, as a result of the relatively broad β-lamellae (about 30 nm) which form coplanar stacks whose plane tends to twist along the growth direction [10,11] endowing β-polypropylene with many performance characteristics, such as improved elongation at break and impact strength [12–20]. While the stable α-structure develops under standard processing conditions, the occurrence of β-form has to be forced by directional crystallization in a temperature gradient field [12,13,21], either by shear-induced crystallization [22–24] or by the addition of specific nucleating agents [25–28]. The latter technique is the most effective and accessible method to obtain *i*-PP with higher level of β-crystal form. The most commonly used nucleating agents are γ-quinacridone (Permanent Red E3B) [29–31], calcium pimelate or suberate [32–34] and *N*,*N*-dicyclohexyl-2,6-naphthalene dicarboxamide produced by New Japan Chemicals – better known as NJ Star NU-100 [35–38]; nevertheless, Huang et al. found that various organic dyes such as Indigosol Brown, Indigosol Red, Indigosol Pink, etc, were all effective *i*-PP β-nucleating agents and led to the production of β-*i*-PP of different β-crystallinities with a *k*-value (fraction of β-phase, k_β) ranging from 0.54 to 0.95 for different nucleators [48].

For inducing β-crystallization in *i*-PP by using β-nucleating agent, the effect of the amount of the nucleating agent is very delicate. Sterzynski et al. studied the nucleation efficiency of *i*-PP nucleated with a β-nucleating agent of Permanent Red E3B thoroughly. It was found that a maximum of *k*-value was obtained for a concentration of 5×10^{-5} wt% of the Permanent Red E3B [30]. Yu et al. investigated the effects of two special polymeric β-nucleating agents (polystyrene (PS) and acrylonitrile–styrene (SAN) copolymer) on the crystallization of *i*-PP [28]. Wide-angle X-ray diffraction (WAXD) results revealed that the k_β values of the two series of nucleated *i*-PP blends first increased with increasing SAN or PS amount, reached

* Corresponding authors. Fax: +86 10 82611905.
E-mail address: jydong@iccas.ac.cn (J.-Y. Dong).

0032-3861/$ – see front matter © 2008 Elsevier Ltd. All rights reserved.
doi:10.1016/j.polymer.2008.09.037

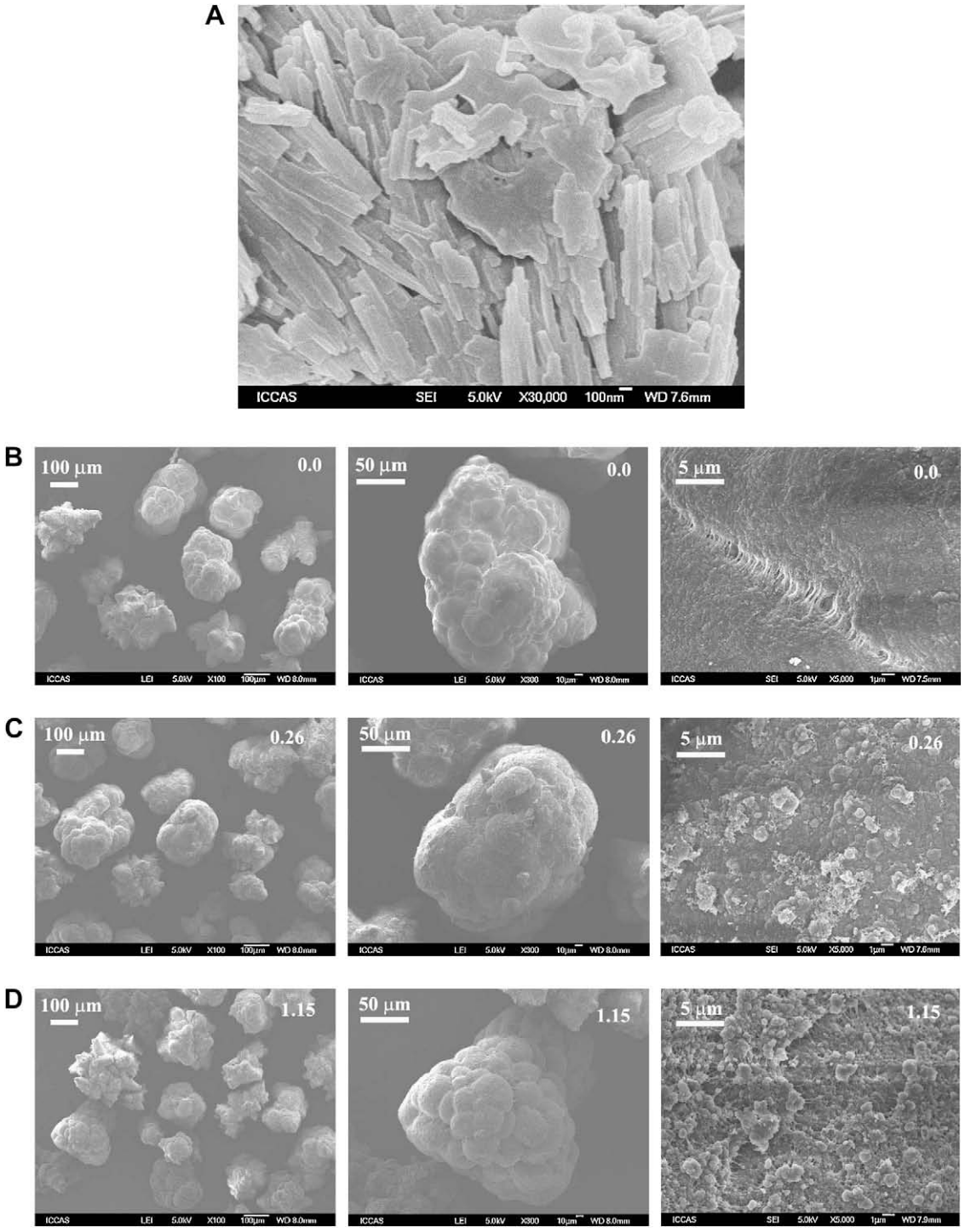

Fig. 1. SEM images of (A) NAβ alone and β-nucleated polypropylene particles with different content of NAβ: (B) 0.0, (C) 0.26 and (D) 1.15 wt%.

a maximum value (when SAN or PS percentage was at about 2%), and then decreased with a further increase of the polymeric nucleating agent percentages. Feng et al. used a hetero-nuclear dimetal complex of lanthanum and calcium (WBG) as a β-nucleating agent for *i*-PP [39]; they investigated the effects of WBG on *i*-PP crystallization behavior and found that the optimum concentration of WBG is at 0.08 wt%. It should be noted that in these literatures the incorporations of the β-nucleating agents into *i*-PP were all based on melt blending. With this classical method, a common scenario can be outlined that, with the increase of the amount of the β-nucleating agent, the nucleation efficiency first increases, and then reaches a maximum before decreasing rather rapidly with a further increase of nucleating agent amount due to agglomeration. Especially, it has been found that the concentration of a non-polymeric nucleating agent beginning to agglomerate was not more than 0.1 wt%. All of these studies lead to the assertions that it is difficult to achieve a rather good dispersion of β-nucleating agent in *i*-PP matrix, and that it is also difficult to reach high levels of β-crystallization due to the limitation on the amount of β-nucleating agent. Under these circumstances, it has generally been necessary to use high energy, rigorously mixing equipment and unduly prolonged mixing cycles in order to avoid visible specks in the finished products and assure

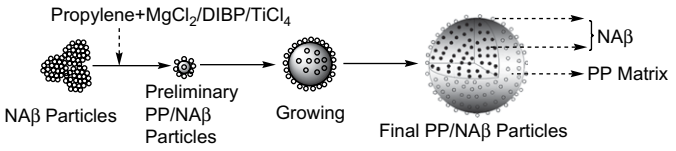

Fig. 2. Schematic representation of the dispersion process of nucleating agent in *i*-PP matrix.

a uniform dispersion of the nucleating agent throughout the entire base polymer.

In this paper, a polymerized dispersion method, namely, nucleating agent dispersing in *i*-PP matrix right through the polymerization of propylene, was employed to comprise a β-nucleating agent, NAβ, a complex of stearic acid and stearate lanthanum in *i*-PP conveniently. The major objective of this work was set to provide a simpler and more economical procedure for achieving a uniform distribution of β-nucleating agent in *i*-PP. The effects of NAβ of different concentrations on the nucleation efficiency of *i*-PP were studied.

2. Experimental part

2.1. Materials

All O_2-moisture-sensitive manipulations were carried out inside an argon-filled vacuum atmosphere dry-box equipped with a dry train. CP grade heptane was deoxygenated by argon purge before refluxing for 48 h and distilling over sodium. Triethylaluminium (TEA) (99.0%) was purchased from Albermarle and used as-received. Dimethoxydiphenylsilane (DDS, 98.5%) and catalyst $MgCl_2$/DIBP/$TiCl_4$ system (Ti content: 2.52 wt%) were kindly supplied by Yingkou Science Chemical Co. (Yingkou, Liaoning province, China). The β-nucleating agent, NAβ, was kindly supplied by Guangdong Winner Functional Materials Co. (Foshan, Guangdong province, China) and was a complex of stearic acid and stearate lanthanum.

2.2. Propylene polymerization

Propylene polymerization reactions were carried out using a Parr stainless-steel autoclave reactor equipped with a mechanical stirrer. In a typical reaction using the $MgCl_2$/DIBP/$TiCl_4$ catalyst, 0.03 g of catalyst (0.016 mmol Ti) was added into the reactor that had been charged with 100 ml heptane, 0.05 g NAβ, 1.8 ml (0.16 mmol) DDS and 0.88 ml (1.58 mmol) TEA under a propylene pressure of 0.5 MPa. After 0.5 h, the reaction was terminated by quenching with 100 ml acidified ethanol (10%). After filtration, repeated washing with ethanol and drying at 60 °C under vacuum, 14.14 g polymer was obtained.

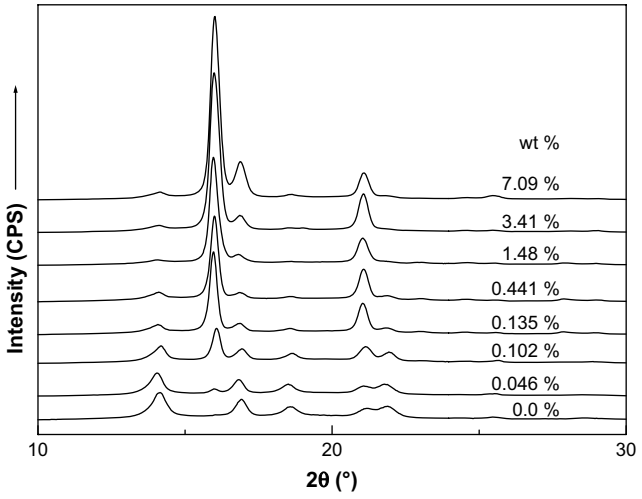

Fig. 3. WAXD diagrams with assigned reflections obtained after completing isothermal crystallization at 135 °C for 2 h.

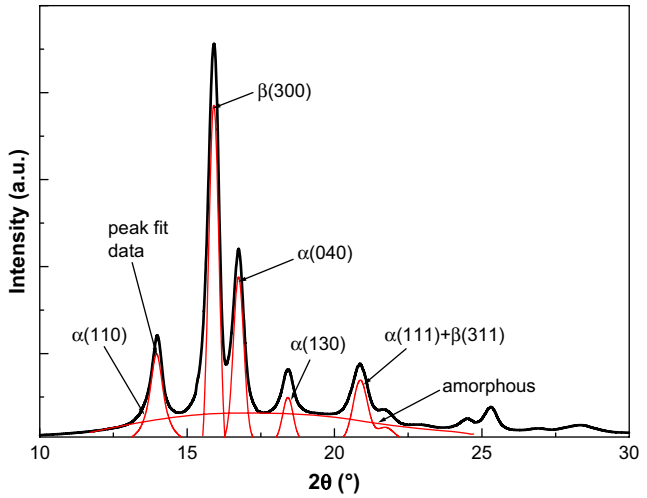

Fig. 4. Deconvolution of an example WAXD intensity profile for the calculation of total crystallinity and contribution of α-form crystal and β-form crystal.

2.3. Instruments and characterization

The determination of the melting and crystallization temperature of the polymers was carried out using differential scanning calorimetry (DSC) with a Perkin–Elmer DSC-7 instrument controller at a heating and cooling rate of 10 °C/min. Temperature and calorimetric scales of DSC were calibrated with indium ($T_m = 156$ °C, melting enthalpy (ΔH_m) = 28.45 J/g). Wide-angle X-ray diffraction (WAXD) was performed on a D8 advance X-ray powder diffractometer (Bruker Co.) with Cu Kα radiation ($\lambda = 0.15406$ nm) at a generator voltage of 40 kV and generator current of 40 mA. The scanned 2θ range was from 1.5° to 40° with a scanning rate of 2°/min. The obtained polymers were examined by Scanning Electron Microscopy (SEM) using a Topcon International Scientific Instruments ISI-SX-40 with secondary electron imaging. Samples were mounted on an aluminum stub and carbon coated to form a conductive coating. The morphologies were investigated by a polarized optical

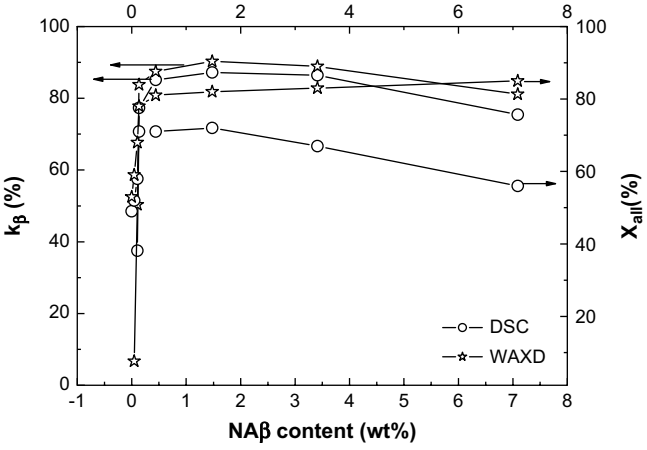

Fig. 5. Relative content of β-crystal form (k_β) and the value of crystallinity (X_{all}), evaluated from DSC and WAXD analyses as a function of the content of NAβ.

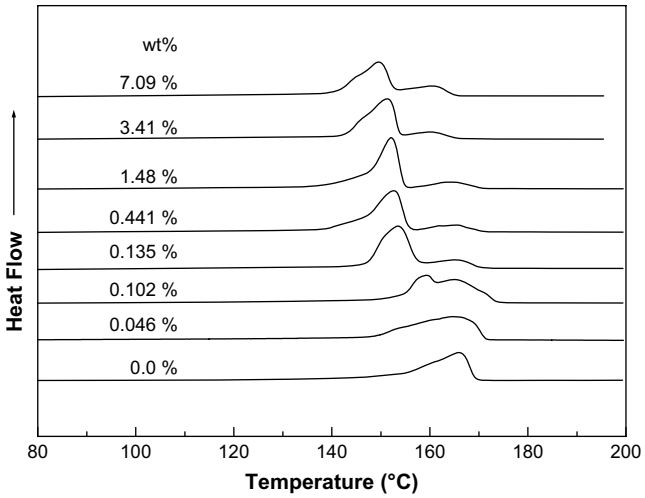

Fig. 6. DSC melting curves measured after isothermal crystallization at 135 °C for 2 h (heating rate: 10 °C/min).

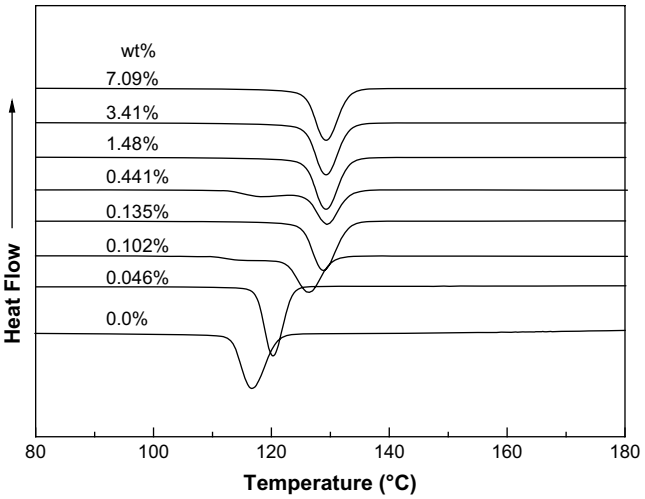

Fig. 8. Crystallization curves of *i*-PP with different concentrations of NAβ.

microscopy (POM) (Linkam Scientific Instruments Ltd., U.K.) equipped with a hot-stage device (CSS-450), a temperature controller and a photo-camera (Nikon-800). To avoid multiple scattering, extremely thin samples, with a nominal thickness of 20.0 μm were prepared by melting the PP films between two glass slides.

3. Results and discussion

3.1. Dispersion of the β-nucleating agent NAβ in i-PP via polymerization

Fig. 1 shows the SEM micrographs of NAβ alone and β-nucleated *i*-PP particles obtained by polymerization method. It can be obviously seen that there are many small particles absorbing on the surface of β-nucleated propylene polymer granules and the number of these particles increase with increasing the content of NAβ. The size of these particles is consistent with that of NAβ, so it can be believed that these particles correspond to NAβ. As we all know that these *i*-PP granules were formed with propylene successively polymerizing on the catalyst surfaces, at the same time, NAβ particles also successively absorbed on the growing *i*-PP polymer granules. This is a dynamic process; finally, NAβ particles were dispersed in *i*-PP matrix evenly. The schematic representation is shown in Fig. 2.

3.2. Effect of the polymerization-dispersed NAβ on i-PP β-crystallization

The relative amounts of different crystal forms in *i*-PP were measured from the X-ray diffraction profiles. In WAXD profiles of *i*-PP, (110) at $2\theta = 14.1°$, (040) at 16.9°, and (130) at 18.5° are the principal reflections of the α-crystal form, while (300) at about 16.0° is the principal reflection of the β-crystal form. These are considered as the characteristic peaks for α-crystals and β-crystals, respectively. The crystallinities and relative contents of different crystal forms of *i*-PP can be calculated from the following equations [16,20,40]:

$$K_\beta = \frac{A_{\beta(300)}}{A_{\alpha(110)} + A_{\alpha(040)} + A_{\alpha(130)} + A_{\beta(300)}} \quad (1)$$

$$X_{all} = 1 - \frac{A_{amorphous}}{\sum A_{amorphous} + A_{crystallization}} \quad (2)$$

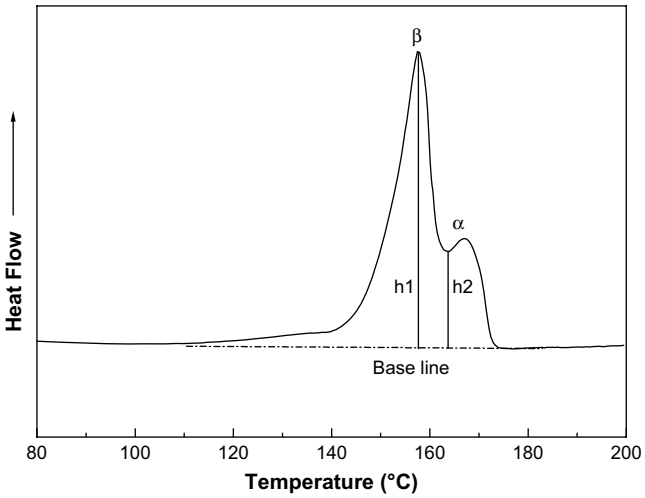

Fig. 7. Schematic plots of calibrated parameters h_1 and h_2.

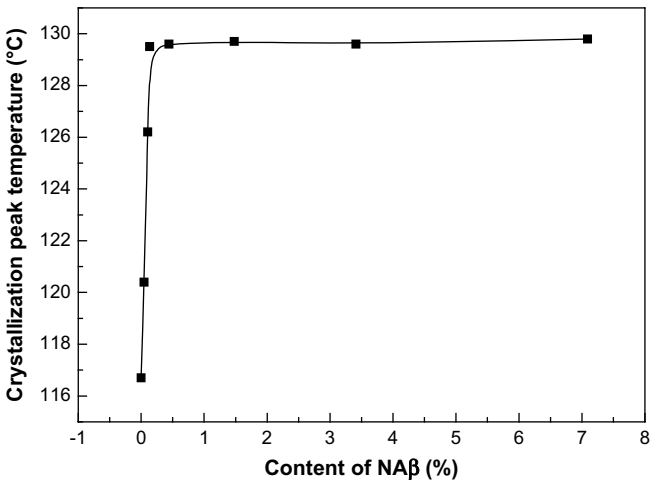

Fig. 9. Dependence of the crystallization peak temperature on the content of NAβ.

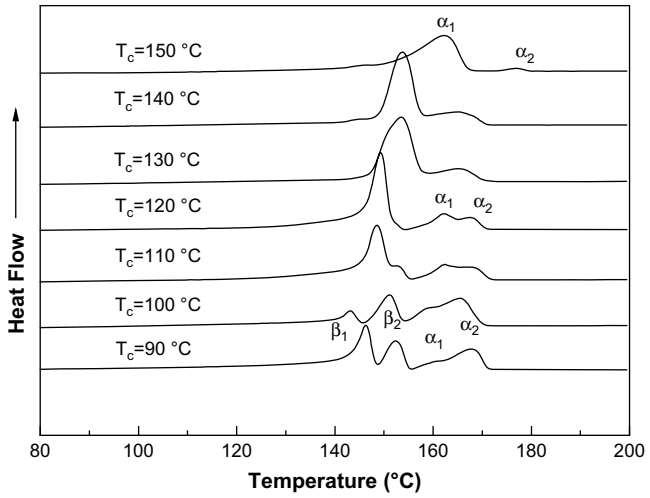

Fig. 10. The effect of crystallization temperature on the DSC melting traces of β-nucleated *i*-PP samples (0.135 wt%, heating rate: 10 °C/min).

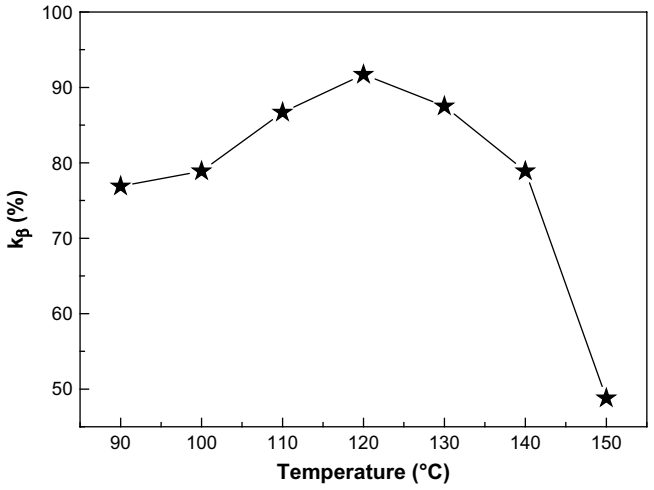

Fig. 12. Relative content of β-crystal form (k_β) evaluated from DSC and WAXD analyses as a function of crystallization temperature.

$$X_\alpha = \left(1 - K_\beta\right) X_{\text{all}} \tag{3}$$

$$X_\beta = K_\beta X_{\text{all}} \tag{4}$$

where K_β expresses the relative amount of the β-crystal phase with respect to the α-crystal phase, $A_{\beta(300)}$ represents the area of the (300) reflection peak, $A_{\alpha(110)}$, $A_{\alpha(040)}$, and $A_{\alpha(130)}$ represent the areas of the (110), (040), (130) reflection peaks, respectively, and $A_{\text{amorphous}}$ is the area of the amorphous peak. A peak-fit procedure was used to deconvolute the peaks of WAXD profiles. A typical profile is shown in Fig. 4. The Gaussian function was used to describe the amorphous and crystal peaks, except for the $\alpha(110)$ peak. The application of the Lorentz function to the $\alpha(110)$ peak is found to give a better fit of whole curve. Fig. 3 shows that the WAXD profiles of NAβ/*i*-PP composites obtained by polymerization method with different NAβ contents isothermally crystallized at 135 °C under quiescent conditions. To compare the crystalline structures of different samples, the WAXD profiles are all plotted at the same intensity scale. It was observed that the WAXD profile of net *i*-PP shows obvious peaks at 2θ of approximate 14.2°, 17.1°, 18.7°, 21.2° and 22.1°, respectively, which correspond to the (110), (040), (130), (131) and (111) reflections. These characteristic diffraction angles indicate that only α-crystal phase exists in the net *i*-PP sample. However, in the WAXD profiles of NAβ/*i*-PP composites even with a low NAβ content, there is an obvious peak at about 15.9° which corresponds to the (300) reflection of β-crystal phase existing in these polymerization samples. k_β values as a function of the content of the β-nucleating agent are reported in Fig. 5. The calculation results show that the k_β value increases with increasing NAβ concentration, reaches a maximum value (88.7%) when NAβ percentage is 0.135 wt%, then holds constant when NAβ percentage is within 3.41 wt%. Only when further increasing the concentration of NAβ would the k_β value decrease. The trend is in contrast with those found in earlier literature reports [28,30,39] obtained on *i*-PP nucleated classically by melt blending where k_β value increased upon the addition of β-nucleating agent, quickly reached a maximum value, and then decreased until constant with increasing of the β-nucleating agent concentration. It could be the reason that polymerization-aided dispersion of NAβ improved the wettability between *i*-PP and NAβ promoting the homogeneous dispersion of NAβ in *i*-PP matrix. Moreover, the aggregation of NAβ particles eased because of the wettability improvement between *i*-PP and NAβ at relatively higher concentrations of β-nucleating agent.

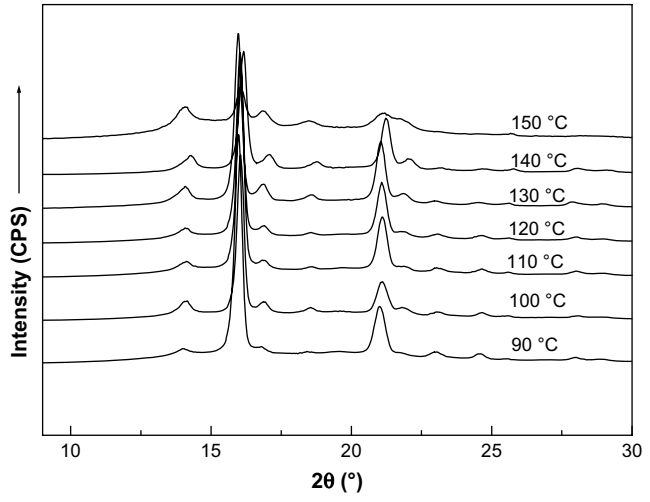

Fig. 11. WAXD diagrams with assigned reflections obtained after completing isothermal crystallizations at different temperatures for 2 h.

For comparison, differential scanning calorimetry (DSC) was used to characterize the contents of β-crystals of the same samples. The DSC curves of *i*-PP with different contents of NAβ are shown in Fig. 6. The melting peak at low temperature is attributed to the β-crystals and that at high temperature belongs to α-crystals. The percentage of β-phase of the samples, β_c, can be obtained from the crystallinities of the α-phase and β-phase according to

$$\phi_\beta = \frac{X_\beta}{X_\beta + X_\alpha} \times 100\% \tag{5}$$

where X_α and X_β are the crystallinities of the α- and β-phases, respectively, and can be calculated separately according to

$$X_i = \frac{\Delta H_i}{\Delta H_i^\theta} \times 100\% \tag{6}$$

where ΔH_i is the calibrated specific fusion heat of either the α- or β-phase which can be obtained through the method by Li and Cheung [34]. ΔH_i^θ is the standard fusion heat of the α- or β-crystals of *i*-PP, being 178 and 170 J/g, respectively [41].

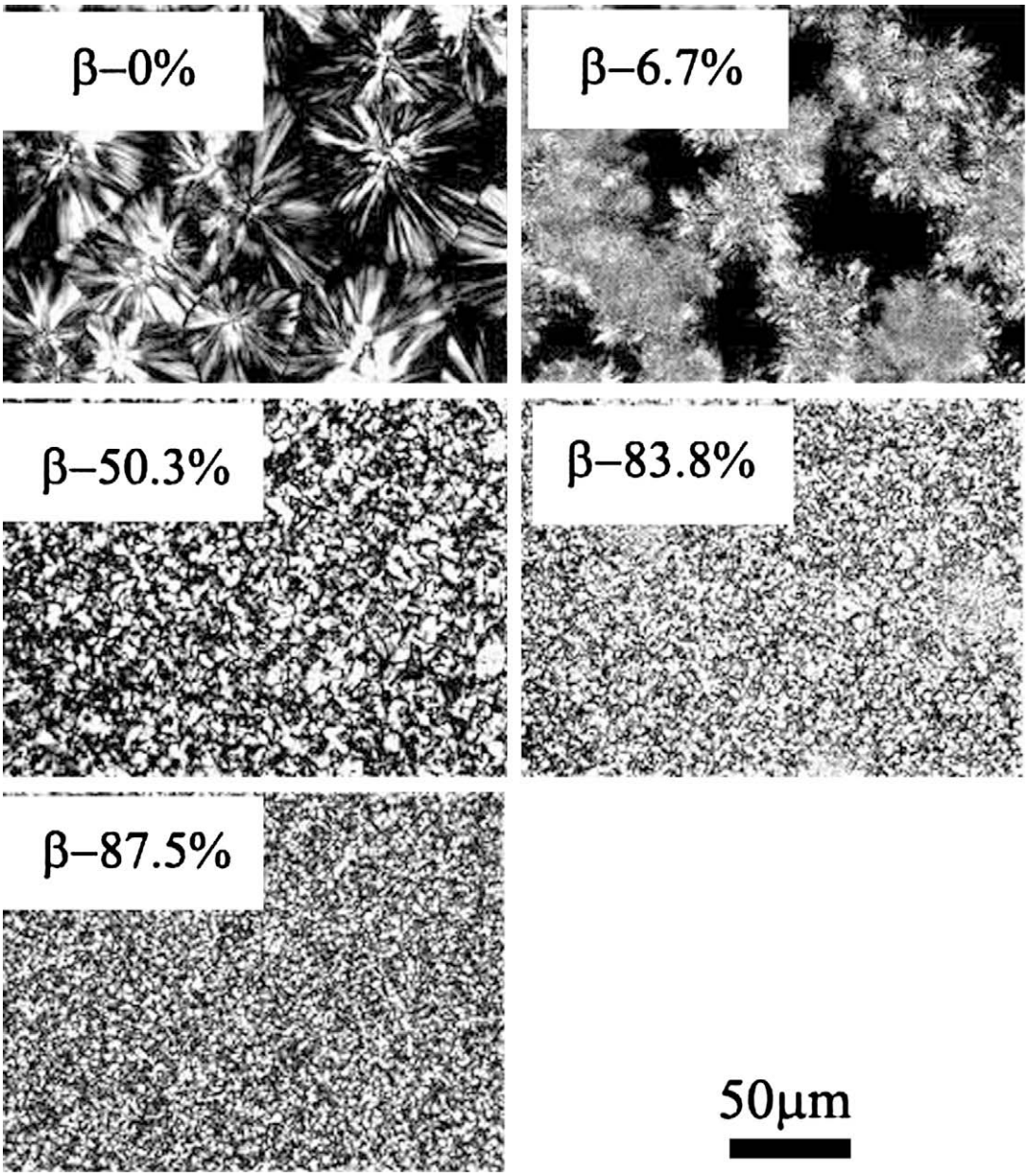

Fig. 13. Evolution of the spherulite structure of *i*-PP with increasing NAβ amounts (from 0 to 0.446 wt%) observed by optical microscopy.

Because the DSC curves of β-nucleated *i*-PP exhibited both α- and β-fusion peaks, the specific fusion heats for α- and β-phases were determined according to the following calibration method. The total fusion heat, Δ*H*, was integrated from 80 to 190 °C on the DSC thermogram. A vertical line was drawn through the minimum between the α- and β-fusion peaks and the total fusion heat was divided into β-component, ΔH_β^* and α-component, ΔH_α^*. Since the less-perfect α-crystals melt before the maximum point during heating and contributed to the ΔH_β^*, the true value of β-fusion heat, ΔH_β, has been approximated by a production of multiplying ΔH_β^* with a calibration factor A [34]:

$$\Delta H_\beta = A \times \Delta H_\beta^* \tag{7}$$

$$A = \left[1 - \frac{h_2}{h_1}\right]^{0.6} \tag{8}$$

$$\Delta H_\alpha = \Delta H - \Delta H_\beta \tag{9}$$

where h_1 and h_2 are the heights from the base line to the β-phase peak and minimum point, respectively. A typical procedure is shown in Fig. 7. As shown in Fig. 5, the relative area of β-crystal melting peaks greatly increases when the content of NAβ is lower than 0.135 wt%, then holds constant when NAβ content is below 3.41 wt%.

Table 1
Sample characterization

Samples	$M_n \times 10^{-4}$	M_w/M_n	NAβ (wt%)	kβ (%)
a	7.94	3.98	0.0	0
b	9.01	4.45	0.061	8.6
c	8.65	4.14	0.135	77.8
d	8.04	4.06	0.283	91.2

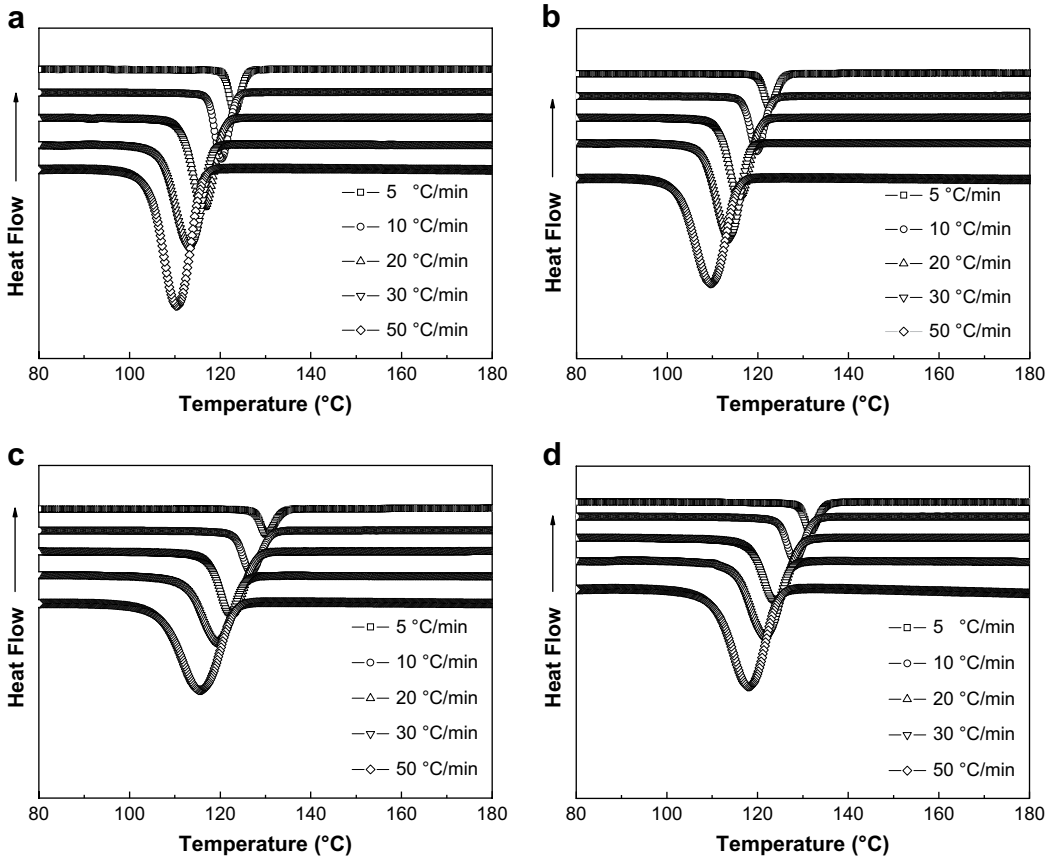

Fig. 14. DSC thermograms of *i*-PP with different concentrations of NAβ.

Only when further increasing the concentration of NAβ will the area of β-crystal melting peaks decrease. The trend is very similar to that from WAXD. However, the k_β value obtained from DSC is 3–10% higher than that from WAXD. One reason is that the exact determination of the β-content is difficult using DSC because the melting peak of the α- and β-phases overlap one another. Another reason is the existing of βα-recrystallization of β-crystals during the melting. Therefore, the WAXD is more accurate than DSC to characterize the content of β-crystals of *i*-PP. According to Eqs. (2) and (5), the values of the total crystallinity (X_{all}), calculated from the X-ray diffraction profiles and DSC curves as shown in Figs. 3 and 6, are reported in Fig. 5 as a function of the content of NAβ. The calculated results from the WAXD diffraction profiles show that the X_{all} values of the samples increase with the increasing NAβ percentage, the maximum value is up to 85%. However, the calculated results from DSC curves show that the X_{all} values of the samples do not increase linearly with the increase of NAβ percentage, reach a maximum value when NAβ percentage is about 0.135 wt%.

3.3. Crystallization behavior

Fig. 8 shows the crystallization behavior of *i*-PP with different contents of NAβ. It is observed that the crystallization peak temperature for *i*-PP is about 116 °C. However, the incorporation of only 0.135 wt% of the β-nucleating agent in *i*-PP produces a marked shift of the crystallization peak toward higher temperature ($T_c = 129.5°$). Fig. 9 shows a plot of T_c as a function of NAβ content. It can be seen that the increase of T_c is very rapid when the content of NAβ is lower than 0.135 wt%, while that is weak when the content of NAβ is higher than 0.2 wt%. It indicates that 0.135 wt% might be the closest to the saturated concentration under the current circumstances, and more nucleating agent would be less effective in increasing the crystallization peak temperature further. Compared with the pure *i*-PP, T_c of *i*-PP with 0.135 wt% NAβ is increased by 12.8 °C.

As aforementioned above, the optimum concentration of NAβ for polymerized *i*-PP/NAβ system in our current study is 0.135 wt%, so this componential *i*-PP/NAβ composite was selected for the study of isothermal crystallization of β-nucleated *i*-PP. Fig. 10 shows the relationship of the contents of β-crystals with the crystallization temperatures. It can be seen that there are four melting peaks when the crystallization temperature is below 120 °C. The first two melting endotherms belong to the β-phases, and the lower endothermic peak is caused by the melting of less stable β_1-crystal phases. The latter two melting endotherms belong to the α-phases, and the lower endothermic peak is caused by the melting of the less stable α_1-crystal phases that was formed during the initial stage of the heating process via βα-recrystallization within the β-phase. When the crystallization temperature is allocated in the range of 130–150 °C ($150\,°C > T_c > 130\,°C$), two distinct melting peaks are observed, the first melting endotherm belonging to the β phase and the second to the α phase. However, if $T_c > 150$ °C, both the endotherms belong to α phase, the first belongs to the disorder-limiting structure (α_1), the other to the order-limiting structure (α_2). For comparison, WAXD was used to characterize the content of β-crystals (k_β) of the same sample. The WAXD profiles of the polymerized *i*-PP/NAβ crystallized at different temperatures are shown in Fig. 11. According to Eq. (1), k_β values were calculated, as shown in Fig. 12. It can be observed that the k_β value first increases, reaches the maximum at 120 °C, then decreases with the further increase of the crystallization temperature. The results show that the β-nucleating ability of NAβ greatly depends on the

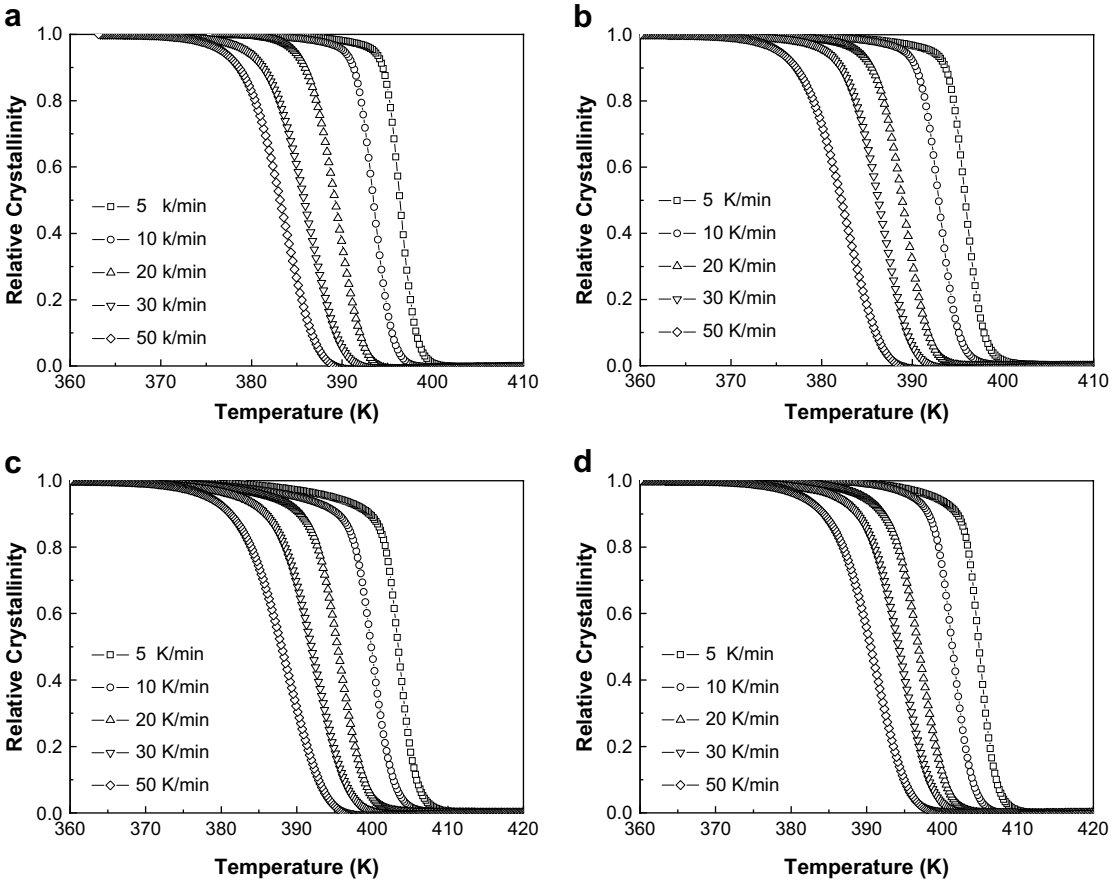

Fig. 15. Plots of X_t versus T for crystallization of *i*-PP with different concentrations of NAβ.

crystallization temperature and there exists an optimum condition. The similar phenomenon was found by Lotz et al. [42].

Polarized optical micrographs of net *i*-PP and polymerized *i*-PP/NAβ compositions with different concentrations of NAβ from 0 to 0.446 wt% crystallized under isothermal conditions are shown in Fig. 13. The 100 μm large α-spherulites disappear progressively, leading to an increasingly finer β-superstructure characterized by spherulites of about 1–5 μm. It is well known that the crystallization process includes the nucleation and the crystal growth. In pure *i*-PP the formation of nuclei is difficult, thus spherulite growth is mainly a homogeneous nucleation, followed by nucleation-controlled spherulite growth. As the nucleation rate is slow and number of nucleus is few, the spherulite of *i*-PP can become very large before it impinges another spherulite. While in β-nucleated *i*-PP, a large number of nuclei would be produced because of the existence of nucleating agent. The nucleation rate is very fast and the spherulite growth in it is a heterogeneous nucleation, followed by a diffusion-controlled growth. Because of the existence of a great deal of nuclei, the spherulites in β-nucleated *i*-PP would be much smaller than those in net *i*-PP.

3.4. Non-isothermal crystallization kinetics

As one of the most important polymorphic materials, *i*-PP exhibits α,β,γ, etc. polymorphs which can have a dramatic impact on the mechanical properties. Therefore, controlling the growth rate and tailoring the proportion of different polymorphs are extremely important for *i*-PP applications. Practical processes usually are under non-isothermal crystallization conditions. In order to find the optimum conditions in practical applications and obtain products with better properties, it is necessary to make a quantitative evaluation on the non-isothermal crystallization process. In this work, three different contents of β-nucleating agent samples were selected for the non-isothermal crystallization study, as shown in Table 1. The non-isothermal crystallization of net *i*-PP and β-nucleated *i*-PP was carried out by DSC with cooling rates from 5.0 to 50 °C/min. The thermograms of net *i*-PP and β-nucleated *i*-PP are plotted in Fig. 14. From these curves, some useful parameters, such as the peak temperature (T_p) and relative crystallinity (X_t) as a function of crystallization temperature can be obtained for describing the non-isothermal crystallization behavior of these selected samples. T_p shifts, as expected, to lower temperature with an increase of cooling rate for all the samples. A shorter time period for the polymer to crystallize will gain as the cooling rate increases; therefore, a higher undercooling is required to initiate crystallization. Besides, the motion of PP molecules might not be able to catch up with the cooling temperature when the specimens were cooled down fast.

The relative degree of crystallinity, X_t, is defined as

$$X_t = \int_{T_0}^{T} (dH_c/dT)dT \Big/ \int_{T_0}^{T_\infty} (dH_c/dT)dT \qquad (10)$$

where T_0 and T_∞ are the onset and end of crystallization temperatures, respectively. Fig. 15 shows the relative degree of crystallinity, X_t, as a function of temperature for net *i*-PP and β-nucleated *i*-PP at various cooling rates. All of the curves had the same sigmoidal shapes, implying that the lag effect of the cooling rate on crystallization was observed only. Using the following

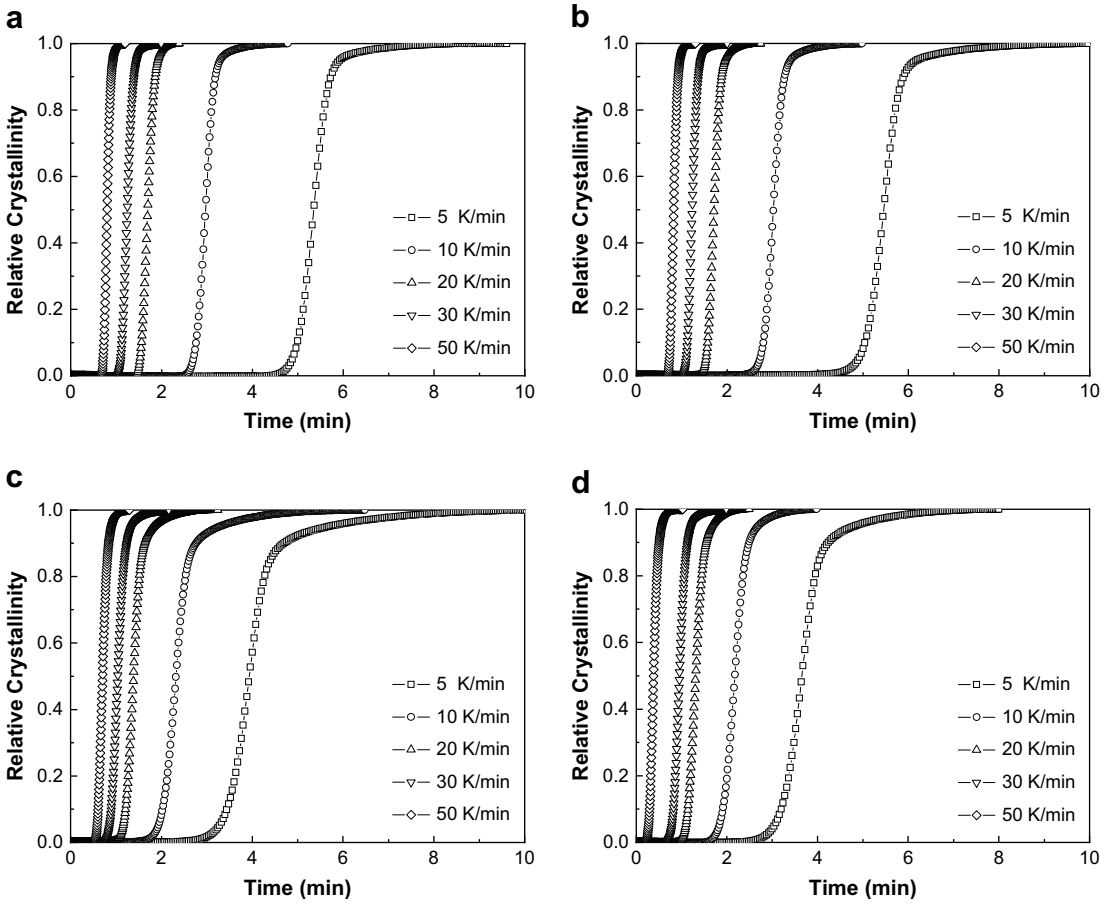

Fig. 16. Plots of X_t versus t for crystallization of *i*-PP with different concentrations of NAβ.

equation, $t = (T_0 - T)/\lambda$ (where T is the temperature at crystallization time t, and λ is the cooling rate), the abscissa of temperature in Fig. 15 could be transformed into a timescale (Fig. 16). The higher the cooling rate, the shorter the crystallization time span. The halftime of non-isothermal crystallization, $t_{1/2}$, was estimated from Fig. 16 for net *i*-PP and β-nucleated *i*-PP, the results listed in Table 2. As expected, the value of $t_{1/2}$ decreases with increasing the cooling rate for all the samples. At some low NAβ contents that are no more than 0.061 wt%, there is negligible difference between the values for the nucleated *i*-PP and net *i*-PP. However, when further increasing NAβ content, $t_{1/2}$ tends to decrease greatly, especially at low cooling rates. It means that the nucleating effect is more significant with increasing the content of NAβ.

As the non-isothermal crystallization is a rate-dependent process, assuming that the polymer melt be cooled at a constant rate, and accounting for the effect of cooling rate on crystallization, Lou and Mo [43] proposed a unique kinetics equation by combining Avrami and Ozawa equations to more accurately describe the non-isothermal crystallization process.

$$\ln\lambda = \ln F(T) - \alpha \ln(t) \tag{11}$$

where kinetic parameter $F(T) = [K(T)/k]^{1/m}$ refers to the cooling rate that needs to be selected within a unit of crystallization time when measured system amounts to a certain degree of crystallinity and α is the ratio of Avrami exponent n to Ozawa exponent m (n/m). The smaller the value of $F(T)$, the higher the crystallization rate becomes. Thus, at a given degree of crystallinity, from the plot of ln λ versus ln t (Fig. 17), the values of α and $F(T)$ can be obtained by the fitting of the linear slopes and the intercepts of the lines, respectively. The results are listed in Table 3. It can be seen that the values of $F(T)$ increase with the increase of the relative crystallinity, indicating that at an unit crystallization time, a higher cooling rate should be required to obtain a higher degree of crystallinity. And at a given degree of crystallinity, the value of $F(T)$ hardly changes compared with that of *i*-PP when the content of NAβ was lower than 0.061 wt%. Further increase of the content of NAβ results in a decrease of the value of $F(T)$. The trend is similar to that of $t_{1/2}$.

Table 2
Half-crystallization time of samples during non-isothermal crystallization process

Cooling rate	$t_{1/2}$ (min)			
	a	b	c	d
5	5.37	5.47	3.94	3.66
10	2.96	3.02	2.31	2.17
20	1.69	1.69	1.39	1.25
30	1.25	1.23	1.05	0.97
50	0.79	0.81	0.69	0.39

3.5. Crystallization activation energy

It is well known that the crystallization of polymers is controlled by two factors: the dynamic factor, which is related to the ΔE value for the transport of crystalline unites across the phase, and the static factor, which is related to the free energy barrier for nucleation. The effective activation energy ΔE for non-isothermal crystallization can be evaluated from Kissinger method [44]. Taking into account the variation of

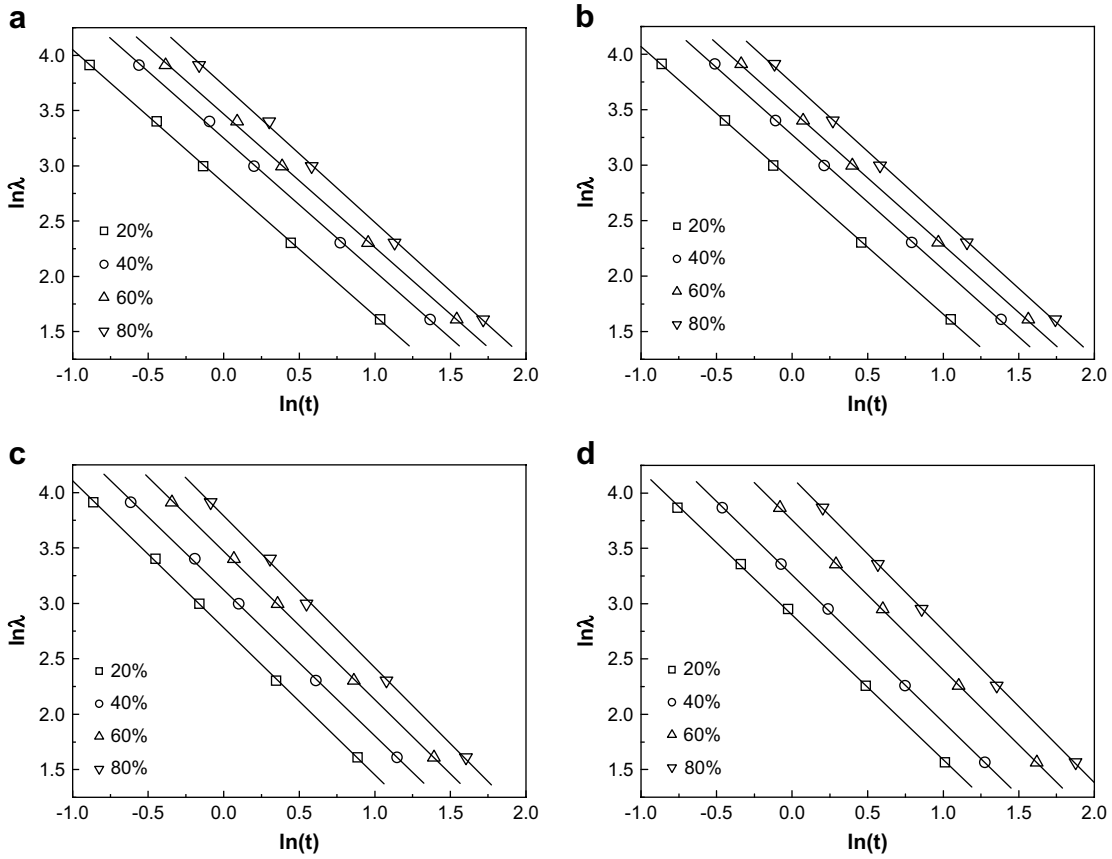

Fig. 17. Plots of ln λ versus ln t for i-PP with different concentrations of NAβ.

the peak temperature T_p with the cooling rate λ the effective activation energy ΔE can be evaluated based on plots of the following form:

$$\frac{d\left[\ln\phi/T_p^2\right]}{d(1/T_p)} = -\frac{\Delta E}{R} \tag{12}$$

where R is the gas constant. Fig. 18 illustrates plots based on the Kissinger method. And it can be seen that good linear relations are obtained. From the slopes of the curves, the effective activation energy ΔE can be calculated accordingly. The calculated values of the activation energy obtained are listed in Table 3. The ΔE of net i-PP and β-nucleated i-PP with 0.061 wt% of NAβ during non-isothermal crystallization is determined to be 260.08 and 256.14 kJ/mol, respectively. It is of almost no difference in ΔE between the two samples. However, ΔE decreases with the NAβ content increases. These results are in contrast to those reported for other nucleating agents [45–47], where the addition of nucleating gents increased the crystallization energy of i-PP due to the weak interaction between the nucleating agents and the segments of i-PP

Table 3
Values of $F(T)$, α, and ΔE for Crystallization of i-PP and β-Nucleated i-PP

Samples	X_t (%)	α	$F(T)$	Activation energy ΔE (kJ/mol)
a	20	1.20	17.24	260.08
	40	1.21	25.81	
	60	1.21	32.09	
	80	1.24	41.65	
b	20	1.21	17.02	256.14
	40	1.21	25.40	
	60	1.21	31.82	
	80	1.23	41.18	
c	20	1.33	10.12	172.25
	40	1.32	16.69	
	60	1.34	25.12	
	80	1.37	36.23	
d	20	1.31	9.96	164.34
	40	1.33	16.20	
	60	1.32	24.72	
	80	1.35	35.58	

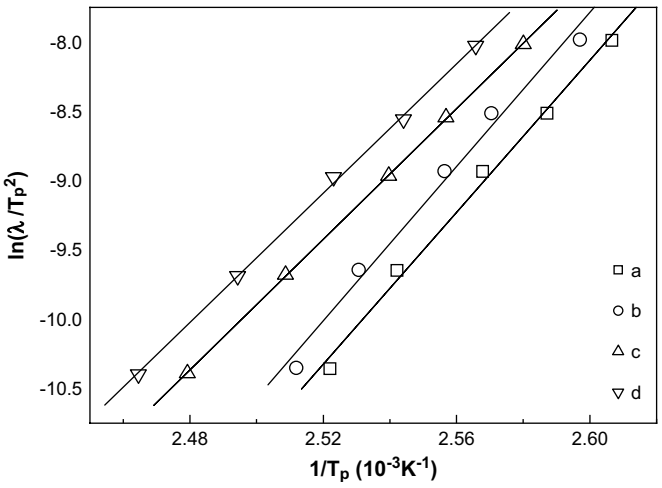

Fig. 18. Kissinger Plots for evaluating non-isothermal crystallization activation energies of i-PP with different concentrations of NAβ.

baffling the transport of macromolecular segments from *i*-PP melts to the crystal growth surface. It suggested that the polymerization–dispersion method promoted the interaction between the nucleating agents and segments of *i*-PP that facilitated the crystal growth process.

4. Conclusions

In this work, a new way for compounding a kind of β-nucleating agent and *i*-PP, namely, polymerization–dispersion method, was proposed. The effects of a polymerized dispersion of the β-nucleating agent on the content of β-crystal, crystallization behavior and non-isothermal crystallization kinetics of *i*-PP were investigated. The main conclusions are summarized as follows.

(1) The k_β value increases with increasing the β-nucleating agent NAβ concentration, reaching a maximum value (88.7%) at 0.135 wt%, then holding constant until 3.41 wt%. The unique effect of NAβ concentration on the k_β value can be interpreted as a result of the profoundly homogeneous dispersion of NAβ in *i*-PP matrix accomplished by the polymerization–dispersion method.
(2) The crystallization behavior studied by DSC and POM shows that the β-nucleating agent NAβ can greatly increase the crystallization peak temperature of *i*-PP, with the spherulite sizes dramatically decreasing with the increase of nucleating agent concentration.
(3) The Mo equation was used to study the non-isothermal crystallization kinetics of *i*-PP with different NAβ concentrations. The result reveals that the introduction of NAβ into *i*-PP greatly increases *i*-PP crystallization rate. The crystallization activation energy was determined by Kissinger method, the results showing that NAβ decreases the crystallization activation energy of *i*-PP. It can be interpreted that a polymerization–dispersion method promotes the interaction between the nucleating agent and *i*-PP matrix, which greatly facilitates the transport of macromolecular segments from *i*-PP melt to the crystal growth surface and reduces the crystallization activation energy.

Acknowledgement

The authors are grateful for financial support from the National Science Foundation of China (Grant no. 20734002).

References

[1] Padden FJ, Keith HD. J Appl Phys 1959;30:1479.
[2] Turner-Jines A, Cobbold AJ. J Polym Sci 1968;B6:539.
[3] Morrow DR, Newman BA. J Appl. Phys. 1968;39:4944.
[4] Meille SV, Bruckner S, Porzio W. Macromolecules 1990;23:4114.
[5] Lotz B, Graff S, Straupe C, Wittmann JC. Polymer 1991;32:2902.
[6] Brückner S, Meille SV, Petraccone V, Pirozzi B. Prog Polym Sci 1991;16:361.
[7] Varga J. J Mater Sci 1992;27:2557.
[8] Lotz B, Wittmann JC, Lovinger AJ. Polymer 1996;37:4979.
[9] Hosemann R, Wilke W. Makromol Chem 1968;118:230.
[10] Norton DR, Keller A. Polymer 1985;26:704.
[11] Keith HD, Padden FJ, Walter NM, Wickhoff HW. J Appl Phys 1959;30:1485.
[12] Fujiwara Y. Colloid Polym Sci 1975;253:273.
[13] Lovinger AJ, Chua JO, Gryte CC. J Polym Sci Polym Phys Ed 1977;15:641.
[14] Vaga J. J Therm Anal 1989;35:1981.
[15] Stocker W, Schumacher M, Graff S, Thierry A, Wittmann JC, Lotz B. Macromolecules 1998;31:807.
[16] Huo H, Jiang SC, An LJ, Feng JC. Macromolecules 2004;37:2478.
[17] Varga J. Angew Makromol Chem 1983;112:191.
[18] Tribout C, Monasse B, Haudin JM. Colloid Polym Sci 1996;274:197.
[19] Somani RH, Hsiao BS, Nogales A, Srinivas S, Tsou AH, Scics I, et al. Macromolecules 2000;33:9385.
[20] Somani RH, Hsiao BS, Nogales A, Fruitwala H, Srinivas S, Tsou AH. Macromolecules 2001;34:5902.
[21] Crissman J. J Polym Sci 1969;7(A2):389.
[22] Devaux E, Chabert B. Polym Commun 1991;32:464.
[23] Varge J, Karger-Kocsis J. Polymer 1995;36:4877.
[24] Ellis G, Gomez MA, Marco C. J Macromol Sci Phys 2004;43:191.
[25] Kawai T, Iijima R, Yamamoto Y, Kimura T. Polymer 2002;43:7301.
[26] Varga J, Mudra I, Ehrenstein GW. J Appl Polym Sci 1999;74:2357.
[27] Krache R, Benavente R, López-Majada JM, Peereña JM, Cerrada ML, Pérez E. Macromolecules 2007;40:6871.
[28] Su ZQ, Dong M, Guo ZX, Yu J. Macromolecules 2007;40:4217.
[29] Garbarczyk J, Paukszta D. Colloid Polym Sci 1985;263:985.
[30] Sterzynski T, Calo P, Lambla M, Thomas M. Polym Eng Sci 1997;37:1917.
[31] Mathieu C, Thierry A, Wittmann IC, Lotz B. J Polym Sci B Polym Phys 2002; 40:2504.
[32] Tjong SC, Shen JS, Li RKY. Polymer 1996;37:2309.
[33] Varga J, Schulek-Toth F. J Therm Anal 1996;47:941.
[34] Li JX, Cheung WL. Polymer 1998;39:6935.
[35] Chu F, Kimura Y. Polymer 1996;37:573.
[36] Busse K, Kressler J, Maier RD, Scherble J. Macromolecules 2000;33:8775.
[37] Nezbedova E, Pospisil V, Bohaty P, Vlach B. Macromol Symp 2001; 170:349.
[38] Scudla J, Raab M, Eichhorn KJ, Strachota A. Polymer 2003;44:4655.
[39] Xiao WC, Wu PY, Feng JC. J Appl Polym Sci 2008;108:3370.
[40] Turner-Jones A, Aiziewood JM, Beckett DR. Macromol Chem 1964;75:134.
[41] Li JX, Cheung WL, Jia D. Polymer 1999;40:1219.
[42] Lotz B, Wittmann JC, Stocker W, Magonov SN, Cantow HJ. Polym Bull 1991; 26:209.
[43] Lou TX, Mo ZS. Acta Polym Sin 1993;1:1.
[44] Kissinger HE. J Res Natl Bur Stand 1956;57:217.
[45] Zhao SC, Cai Z, Xin Z. Polymer 2008;49:2745.
[46] Zhang YF, Xin Z. J Appl Polym Sci 2006;101:3307.
[47] Jang GS, Cho WJ, Ha CS. J Polym Sci B Polym Phys 2001;39:1001.
[48] Huang MR, Li XG, Fang BR. J Appl Polym Sci 1995;56:1323.